

Spectral Synthesis of SDSS Galaxies

L. Sodré Jr.¹, R. Cid Fernandes², A. Mateus¹, G. Stasińska³, J. M. Gomes²

¹*Instituto de Astronomia, Geofísica e Ciências Atmosféricas,
Universidade de São Paulo, São Paulo, SP, Brazil*

²*Depto. de Física - CFM - Universidade Federal de Santa Catarina, SC,
Brazil*

³*LUTH, Observatoire de Meudon, 92195 Meudon Cedex, France*

Abstract. We investigate the power of spectral synthesis as a mean to estimate physical properties of galaxies. Spectral synthesis is nothing more than the decomposition of an observed spectrum in terms of a superposition of a base of simple stellar populations of various ages and metallicities (here from Bruzual & Charlot 2003), producing as output the star-formation and chemical histories of a galaxy, its extinction and velocity dispersion. We discuss the reliability of this approach and apply it to a volume limited sample of 50362 galaxies from the SDSS Data Release 2, producing a catalog of stellar population properties. Emission lines are also studied, their measurement being performed after subtracting the computed starlight spectrum from the observed one. A comparison with recent estimates of both observed and physical properties of these galaxies obtained by other groups shows good qualitative and quantitative agreement, despite substantial differences in the method of analysis. The confidence in the method is further strengthened by several empirical and astrophysically reasonable correlations between synthesis results and independent quantities. For instance, we report the existence of strong correlations between stellar and nebular metallicities, stellar and nebular extinctions, mean stellar age and equivalent width of H α and 4000 Å break, and between stellar mass and velocity dispersion. We also present preliminary results of an analysis of a magnitude-limited sample which clearly reveals that the bimodality of galaxy populations is present in the parameters computed in the synthesis. Our results are also consistent with the “down-sizing” scenario of galaxy formation and evolution. Finally, we point out one of the major problems facing spectral synthesis of early-type systems: the spectral base adopted here is based on solar-scaled evolutionary tracks whose abundance pattern may not be appropriate for this type of galaxy.

1. Introduction

In the proceedings of the meeting on Stellar Populations held in Baltimore in 1986 Searle (1986), discussing integral light spectral synthesis, states that “this subject has a bad reputation. Too much has been claimed, and too few have been persuaded”. Indeed, recovering the stellar content of a galaxy from its observed integrated spectrum is not an easy task, as can be deduced from the amount of work devoted to this topic over the past half century. The situation is however much more favorable nowadays. Huge observational and theoretical efforts in the past few years have produced large sets of high quality spectra

of stars (e.g., Prugniel & Soubiran 2001; Le Borgne et al. 2003; Bertone et al. 2004; González-Delgado et al. 2005). These libraries are being implemented in a new generation of evolutionary synthesis models, allowing the prediction of galaxy spectra with an unprecedented level of detail (Vazdekis 1999; Bruzual & Charlot 2003, hereafter BC03; Le Borgne et al. 2004). At the same time, galaxy spectra are now more abundant than ever. The Sloan Digital Sky Survey (SDSS), in particular, is providing a homogeneous data base of hundreds of thousands of galaxy spectra in the 3800–9200 Å range, with a resolution of $\lambda/\Delta\lambda \sim 1800$ (York et al. 2000; Stoughton et al. 2002; Abazajian et al. 2003, 2004). This enormous amount of high quality data will undoubtedly be at the heart of tremendous progress in our understanding of galaxy constitution, formation and evolution. Actually, galaxy spectra encode information on the age and metallicity distributions of the constituent stars, which in turn reflect the star-formation and chemical histories of the galaxies. Retrieving this information from observational data in a reliable way is crucial for a deeper understanding of galaxy formation and evolution and, in fact, significant steps in this direction have recently been made (Kauffmann et al. 2003a, hereafter K03; Brinchmann et al. 2004; Tremonti et al. 2004; Heavens et al. 2004; Panter, Heavens & Jimenez 2004).

Here we demonstrate that, besides providing excellent starlight templates to aid emission line studies, spectral synthesis recovers reliable stellar population properties out of galaxy spectra of realistic quality. We show that this simple method provides robust information on the stellar age (t_*) and stellar metallicities (Z_*) distributions, as well as on the extinction, velocity dispersion and stellar mass. The ability to recover information on Z_* is particularly welcome, given that stellar metallicities are notoriously more difficult to assess than other properties. In order to reach this goal we follow: (1) *a priori* arguments, based on simulations; (2) comparisons with independent work based on a different method, and (3) an *a posteriori* empirical analysis of the consistency of results obtained for a large sample of SDSS galaxies. Most of the results presented here are discussed in detail in Cid Fernandes et al. (2005).

In Section 2 we present an overview of our synthesis method and simulations designed to test it and evaluate the uncertainties involved. The discussion is focused on how to use the synthesis to derive robust estimators of physically interesting stellar population properties. Section 3 defines a volume limited sample of SDSS galaxies and presents the results of the synthesis of their spectra, along with measurements of emission lines. We also compare in this section our results to those obtained by other authors. Stellar population and emission line properties are used in Section 4 to investigate whether the synthesis produces astrophysically plausible results. In Section 5 we present preliminary results of an analysis of a magnitude-limited sample of 20000 galaxies also extracted from SDSS. Finally, Section 6 summarizes our main findings.

2. Spectral Synthesis

2.1. Method

Our synthesis code, which we call STARLIGHT, was first discussed in Cid Fernandes et al. (2004, hereafter CF04). We fit an observed spectrum O_λ with

a combination of N_* Simple Stellar Populations (SSP) from the evolutionary synthesis models of BC03. Extinction is modeled as due to foreground dust, and parametrized by the V-band extinction A_V . The Galactic extinction law of Cardelli, Clayton & Mathis (1989) with $R_V = 3.1$ is adopted. Line of sight stellar motions are modeled by a Gaussian distribution G centered at velocity v_* and with dispersion σ_* . With these assumptions the model spectrum is given by

$$M_\lambda = M_{\lambda_0} \left[\sum_{j=1}^{N_*} x_j b_{j,\lambda} r_\lambda \right] \otimes G(v_*, \sigma_*) \quad (1)$$

where $b_{j,\lambda}$ is the spectrum of the j^{th} SSP normalized at λ_0 , $r_\lambda \equiv 10^{-0.4(A_\lambda - A_{\lambda_0})}$ is the reddening term, M_{λ_0} is the synthetic flux at the normalization wavelength, \vec{x} is the *population vector* and \otimes denotes the convolution operator. Each component x_j ($j = 1 \dots N_*$) represents the fractional contribution of the SSP with age t_j and metallicity¹ Z_j to the model flux at λ_0 . The base components can be equivalently expressed as a mass fractions vector $\vec{\mu}$. In this work we adopt a base with $N_* = 45$ SSPs, encompassing 15 ages between 10^6 and 1.3×10^{10} yr and 3 metallicities: $Z = 0.2, 1$ and $2.5 Z_\odot$. Their spectra were computed with the STELIB library (Le Borgne et al. 2003), Padova 1994 tracks, and Chabrier (2003) IMF (see BC03 for details).

The fit is carried out with a simulated annealing plus Metropolis scheme which searches for the minimum $\chi^2 = \sum_\lambda [(O_\lambda - M_\lambda) w_\lambda]^{-2}$, where w_λ^{-1} is the error in O_λ . Regions around emission lines, bad pixels or sky residuals are masked out by setting $w_\lambda = 0$. Pixels which deviate by more than 3 times the rms between O_λ and an initial estimate of M_λ are also given zero weight.

Fig. 1 illustrates the spectral fit obtained for a galaxy drawn from the SDSS database. The top-left panel shows the observed spectrum (thin line) and the model (thick), as well as the error spectrum (dashed). The bottom-left panel shows the $O_\lambda - M_\lambda$ residual spectrum, while the panels in the right summarize the derived star-formation history encoded in the age-binned population vector. This example, along with those in K03 and CF04, demonstrates that this simple method is capable of reproducing real galaxy spectra to an excellent degree of accuracy.

An important application of the synthesis is to measure emission lines from the residual spectrum, as done by K03. Another, of course, is to infer stellar population properties from the fit parameters. Our central goal here is to investigate whether spectral synthesis can also recover reliable stellar population properties. In the remainder of this section we address this issue by means of simulations.

2.2. Robust description of the synthesis results

The existence of multiple solutions is an old known problem in stellar population synthesis, and even superb spectral fits as that shown in Fig. 1 do not guarantee

¹In this paper we follow the convention used in stellar evolution studies, which define stellar metallicities in terms of the fraction of mass in metals. In this system the Sun has $Z_* = 0.02$.

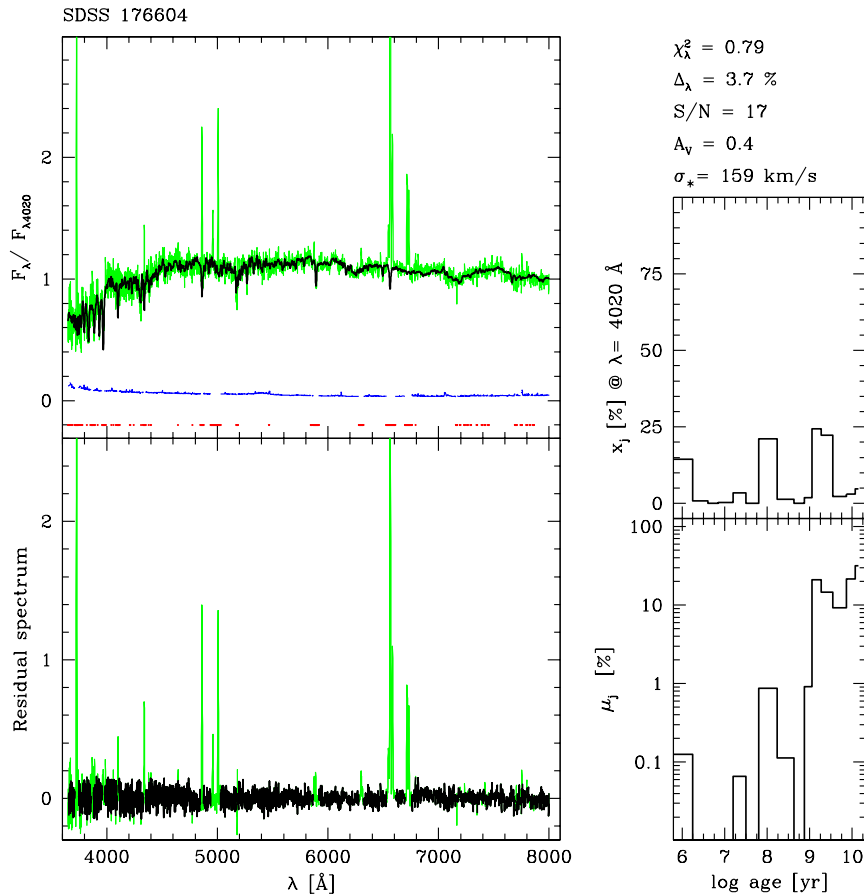


Figure 1. Spectral synthesis of a late type SDSS galaxy. Top-left: Observed (thin line), model (thick line) and error spectra (dashed line). Points along a horizontal line in the bottom of this panel indicate bad pixels (as given by the SDSS flag) or emission lines windows, both of which were masked out in the fits. Bottom-left: Residual spectrum. Masked regions are plotted with a lighter thin line. Right: Flux (top) and mass (bottom) fractions as a function of age. Some of the derived properties are listed in the top-right. χ^2_λ is the reduced χ^2 , and Δ_λ is the mean relative difference between model and observed spectra; S/N refers to the region around $\lambda_0 = 4020$ Å.

that the resulting parameter estimates are trustworthy. There is, consequently, a need to assess the degree to which one can trust the parameters involved in the fit before using them to infer stellar populations properties. The spectral fits involve $N_* + 3$ parameters: $N_* - 1$ of the \vec{x} components (one degree of freedom is removed by the normalization constraint), M_{λ_0} , A_V and the two kinematical parameters, v_* and σ_* . The reliability of parameter estimation is best studied by means of simulations which feed the code with spectra generated with known

parameters, add noise, and then examine the correspondence between input and output values.

Simulations We have carried out simulations designed to test the method and investigate which combinations of the parameters provide robust results. Several sets of simulations were performed. Given our interest in modeling SDSS galaxies, here we focus on simulations tailored to match the characteristics of this data set. Test galaxies were built from the average \vec{x} , A_V and σ_* within 65 boxes in the mean stellar age versus mean stellar metallicity plane obtained for the sample described in Section 3. These new simulations confirm previous results reported in CF04 that the individual components of \vec{x} are very uncertain, so we skip a detailed comparison between \vec{x}_{input} and \vec{x}_{output} and jump straight to results based on more robust descriptions of the synthesis output.

Condensed population vector A coarse but robust description of the star-formation history of a galaxy may be obtained by binning \vec{x} onto “Young” ($t_j < 10^8$ yr), “Intermediate-age” ($10^8 \leq t_j \leq 10^9$ yr), and “Old” ($t_j > 10^9$ yr) components (x_Y , x_I and x_O respectively). These age-ranges were defined on the basis of the simulations, by seeking which combinations of x_j ’s produce smaller input – output residuals. Our simulations show that these 3 components are very well recovered by the method, with uncertainties smaller than $\Delta x_Y = 0.05$, $\Delta x_I = 0.1$, and $\Delta x_O = 0.1$ for $S/N \geq 10$.

Mass, extinction and velocity dispersion We have also analyzed the input versus output values of A_V , σ_* and the stellar mass M_* . The latter is not an explicit input parameter of the models, but may be computed from $\vec{\mu}$ and the M_*/L_{λ_0} ratio of the different populations in the base. The uncertainties in the recovery of these parameters are $\Delta A_V < 0.05$ mag, $\Delta \log M_* < 0.1$ dex and $\Delta \sigma_* < 12$ km s⁻¹ for $S/N \geq 10$.

Mean stellar age If one had to choose a single parameter to characterize the stellar population mixture of a galaxy, the option would certainly be its mean age. We define two versions of mean stellar age (the logarithm of the age, actually), one weighted by light

$$\langle \log t_* \rangle_L = \sum_{j=1}^{N_*} x_j \log t_j \quad (2)$$

and another weighted by stellar mass

$$\langle \log t_* \rangle_M = \sum_{j=1}^{N_*} \mu_j \log t_j \quad (3)$$

Note that, by construction, both definitions are limited to the 1 Myr–13 Gyr range spanned by the base. The mass weighted mean age is in principle more physical, but, because of the non-constant M/L of stars, it has a much less direct relation with the observed spectrum than $\langle \log t_* \rangle_L$.

The simulations show that the mean age is a very robust quantity. The rms difference between input and output $\langle \log t_* \rangle_L$ values is ≤ 0.08 dex for

$S/N > 10$, and ≤ 0.14 dex for $\langle \log t_\star \rangle_M$. Although the uncertainties of $\langle \log t_\star \rangle_L$ and $\langle \log t_\star \rangle_M$ are comparable in absolute terms, the latter index spans a smaller dynamical range (because of the large M/L ratio of old populations), so in practice $\langle \log t_\star \rangle_L$ is the more useful of the two indices.

Mean stellar metallicity Given an option of what to choose as a second parameter to describe a mixed stellar population, the choice would likely be its typical metallicity. Analogously to what we did for ages, we define both light and mass-weighted mean stellar metallicities:

$$\langle Z_\star \rangle_L = \sum_{j=1}^{N_\star} x_j Z_j \quad (4)$$

and

$$\langle Z_\star \rangle_M = \sum_{j=1}^{N_\star} \mu_j Z_j \quad (5)$$

both of which are bounded by the 0.2–2.5 Z_\odot base limits. Our simulations show that the rms of $\Delta \log \langle Z_\star \rangle_M = \log \langle Z_\star \rangle_{M,\text{output}} - \log \langle Z_\star \rangle_{M,\text{input}}$ is of order 0.1 dex. In absolute terms this is comparable to $\Delta \langle \log t_\star \rangle$, but note that $\langle Z_\star \rangle$ covers a much narrower dynamical range than $\langle \log t_\star \rangle$, so that in practice mean stellar metallicities are more sensitive to errors than mean ages. This is not surprising, given that age is the main driver of variance among SSP spectra, metallicity having a “second-order” effect (e.g., Schmidt et al. 1991; Ronen, Aragon-Salamanca & Lahav 1999). This is the reason why studies of the stellar populations of galaxies have a much harder time estimating metallicities than ages, to the point that one is often forced to bin-over the Z information and deal only with age-related estimates such as $\langle \log t_\star \rangle$ (e.g., Cid Fernandes et al. 2001; Cid Fernandes, Le o & Rodrigues Lacerda 2003; K03).

Notwithstanding these notes, it is clear that uncertainties of ~ 0.1 dex in $\langle Z_\star \rangle$ are actually good news, since they do allow us to recover useful information on an important but hard to measure property. This new tracer of stellar metallicity is best applicable to large samples of galaxies such as the SDSS. The statistics of samples help reducing uncertainties associated with $\langle Z_\star \rangle$ estimates for single objects and allows one to investigate correlations between $\langle Z_\star \rangle$ and other galaxy properties (Sodr  et al. , in preparation; Section 4.1.).

Age-Metallicity degeneracy Our method tends to underestimate $\langle Z_\star \rangle$ for metal-rich systems and vice-versa. This trend is due to the infamous age-metallicity degeneracy. In order to verify to which degree our synthesis is affected by this well known problem (e.g., Renzini & Buzzoni 1986; Worthey 1994; Bressan, Chiosi & Tantalo 1996) we have examined the correlation between the output minus input residuals in $\langle \log t_\star \rangle_L$ and $\log \langle Z_\star \rangle_L$. The age- Z degeneracy acts in the sense of confusing old, metal-poor systems with young, metal-rich ones and vice-versa, which should produce anti-correlated residuals. This anti-correlation is also present with the mass-weighted mean stellar metallicity $\langle Z_\star \rangle_M$, but is not as strong as for $\langle Z_\star \rangle_L$. On the other hand, the uncertainty in $\langle Z_\star \rangle_M$ is always larger than for $\langle Z_\star \rangle_L$.

The age- Z degeneracy is thus present in our method, introducing correlated residuals in our $\langle Z_\star \rangle$ and $\langle \log t_\star \rangle$ estimates at the level of up to ~ 0.1 – 0.2 dex. However, none of the results reported here rely on this level of precision.

Base limitations We have carried out simulations using the $Z = 0.02Z_\odot$ BC03 SSPs to examine some of the limitations of the base adopted here. Galaxies with such low metallicity are not expected to be present in significant numbers in the sample described in Section 3.1., given that it excludes low luminosity systems like HII galaxies and dwarf ellipticals (which are also the least metallic ones by virtue of the mass-metallicity relation). Still, it is interesting to investigate what would happen in this case. When synthesized with our 0.2 – $2.5Z_\odot$ base, these extremely metal poor galaxies are modeled predominantly with the $0.2Z_\odot$ components, as intuitively expected. Moreover, the mismatch in metallicity introduces non-negligible biases in other properties, like masses, mean ages and extinction (M_\star , for instance, is systematically underestimated by 0.3 dex). Similar problems should be encountered when modeling systems with $Z > 2.5Z_\odot$. These results serve as a reminder that our base spans a wide but finite range in stellar metallicity, and that extrapolating these limits has an impact on the derived physical properties. While there is no straightforward *a priori* diagnostic of which galaxies violate these limits, in general, one should be suspicious of objects with mean Z_\star too close to the base limits.

Our simulations demonstrate that we are able of producing reliable estimates of several parameters of astrophysical interest, at least in principle. We must nevertheless emphasize that this conclusion relies entirely on models and on an admittedly simplistic view of galaxies. When applying the synthesis to real galaxy spectra, a series of other effects come into play. For instance, the extinction law appropriate for each galaxy likely differs from the one used here. Similarly, while in the evolutionary tracks adopted here the metal abundances are scaled from the solar values, non-solar abundance mixtures are known to occur in stellar systems (e.g., Trager et al. 2000a,b; see also Section 5), not to mention uncertainties in the SSP models and the always present issue of the IMF. Accounting for all these effects in a consistent way is not currently feasible. We mention these caveats not to dismiss simple models, but to highlight that all parameter uncertainties discussed above are applicable within the scope of the model.

Hence, while the simulations lend confidence to the synthesis method, one might remain skeptical of its actual power. The next sections further address the reliability of the synthesis, this time from a more empirical perspective.

3. Analysis of a volume-limited galaxy sample

In this section we apply our synthesis method to a large sample of SDSS galaxies to estimate their stellar population properties. We also present measurements of emission line properties, obtained from the observed minus synthetic spectra. The information provided by the synthesis of so many galaxies allows one to address a long menu of astrophysical issues related to galaxy formation and evolution. Before venturing in the exploration of such issues, however, it is important to validate the results of the synthesis by as many means as possible.

Hence, the goal of this study is not so much to explore the physics of galaxies but to provide an empirical test of our synthesis method.

3.1. Sample definition

The spectroscopic data used in this work were taken from the SDSS. This survey provides spectra of objects in a large wavelength range (3800–9200 Å) with mean spectral resolution $\lambda/\Delta\lambda \sim 1800$, taken with 3 arcsec diameter fibers. The most relevant characteristic of this survey for our study is the enormous amount of good quality, homogeneously obtained spectra. The data analyzed here were extracted from the SDSS main galaxy sample available in the Data Release 2 (DR2; Abazajian et al. 2004). This flux-limited sample consists of galaxies with reddening-corrected Petrosian r -band magnitudes $r \leq 17.77$, and Petrosian r -band half-light surface brightnesses $\mu_{50} \leq 24.5$ mag arcsec⁻² (Strauss et al. 2002).

From the main sample, we first selected spectra with a redshift confidence ≥ 0.35 . Following the conclusions of Zaritsky, Zabludoff, & Willick (1995), we have imposed a redshift limit of $z > 0.05$ (trying to avoid aperture effects and biases; see e.g. Gómez et al. 2003) and selected a volume limited sample up to $z = 0.1$, corresponding to a r -band absolute magnitude limit of $M(r) = -20.5$. The absolute magnitudes used here are k -corrected with the help of the code provided by Blanton et al. (2003; `kcorrect v3.2`) and assuming the following cosmological parameters: $H_0 = 70$ km s⁻¹ Mpc⁻¹, $\Omega_M = 0.3$ and $\Omega_\Lambda = 0.7$. We also restricted our sample to objects for which the observed spectra show a S/N ratio in g , r and i bands greater than 5. These restrictions leave us with a volume limited sample containing 50362 galaxies, which leads to a completeness level of ~ 98.5 per cent.

3.2. Results of the spectral synthesis

All 50362 spectra were brought to the rest-frame (using the redshifts in the SDSS database), sampled from 3650 to 8000 Å in steps of 1 Å, corrected for Galactic extinction² using the maps given by Schlegel, Finkbeiner & Davis (1998) and the extinction law of Cardelli et al. (1989, with $R_V = 3.1$), and normalized by the median flux in the 4010–4060 Å region. The S/N ratio in this spectral window spans the 5–30 range, with median value of 14. Besides the masks around the lines listed in Section 2.2., we exclude points with SDSS flag ≥ 2 , which signals bad pixels, sky residuals and other artifacts. After this pre-processing, the spectra are fed into the STARLIGHT code described in Section 2.1.. On average, the synthesis is performed with $N_\lambda = 3677$ points, after discounting the ones which are clipped by our ≤ 3 sigma threshold (typically 40 points) and the masked ones. The spectral fits are generally very good.

The total stellar masses of the galaxies were obtained from the stellar masses derived from the spectral synthesis (which correspond to the light entering the fibers) by dividing them by $(1 - f)$, where f is the fraction of the total galaxy luminosity in the z -band outside the fiber. This approach, which neglects stellar

²Unlike in the first data release, the final calibrated spectra from the DR2 are not corrected for foreground Galactic reddening.

population and extinction gradients, leads to an increase of typically 0.5 in $\log M_*$. We did not apply any correction to the velocity dispersion estimated by the code given that the spectral resolution of the BC03 models and the data are very similar.

We point out that we did not constrain the extinction A_V to be positive. There are several reasons for this choice: (a) some objects may be excessively dereddened by Galactic extinction; (b) some objects may indeed require bluer SSP spectra than those in the base; (c) the observed light may contain a scattered component, which would induce a bluening of the spectra not taken into account by the adopted pure extinction law; (d) constraining A_V to have only positive values produces an artificial concentration of solutions at $A_V = 0$, an unpleasant feature in the A_V distribution. Interestingly, most of the objects for which we derive negative A_V (typically -0.1 to -0.3 mag) are early-type galaxies. These galaxies are dominated by old populations, and expected to contain little dust. This is consistent with the result of K03, who find negative extinction primarily in galaxies with a large $D_n(4000)$. The distribution of A_V for these objects, which can be selected on the basis of spectral or morphological properties, is strongly peaked around $A_V = 0$, so that objects with $A_V < 0$ can be considered as consistent with having zero extinction. In any case, none of the results reported in this paper is significantly affected by this choice.

3.3. Emission line measurements

Besides providing estimates of stellar population properties, the synthesis models allow the measurement of emission lines from the “pure-emission”, starlight subtracted spectra ($O_\lambda - M_\lambda$). We have measured the lines of [O II] $\lambda\lambda 3726, 3729$, [O III] $\lambda 4363$, H β , [O III] $\lambda\lambda 4959, 5007$, [O I] $\lambda 6300$, [N II] $\lambda 6548$, H α , [N II] $\lambda 6584$ and [S II] $\lambda\lambda 6717, 6731$. Each line was treated as a Gaussian with three parameters: width, offset (with respect to the rest-frame central wavelength), and flux. Lines from the same ion were assumed to have the same width and offset. We have further imposed [O III] $\lambda 5007$ /[O III] $\lambda 4959 = 2.97$ and [N II] $\lambda 6584$ /[N II] $\lambda 6548 = 3$ flux ratio constraints. Finally, we consider a line to have significant emission if its fit presents a S/N ratio greater than 3.

In some of the following analysis, galaxies with emission lines are classified according to their position in the [O III]/H β versus [N II]/H α diagram proposed by Baldwin, Phillips & Terlevich (1981) to distinguish normal star-forming galaxies from galaxies containing active galactic nuclei (AGN). We define as normal star-forming galaxies those galaxies that appear in this diagram and are below the curve defined by K03 (see also Brinchmann et al. 2004). Objects above this curve are transition objects and galaxies containing AGN.

3.4. Comparisons with the MPA/JHU database

The SDSS database has been explored by several groups, using different approaches and techniques. The MPA/JHU group has recently publicly released catalogues³ of derived physical properties for 211894 SDSS galaxies, including 33589 narrow-line AGN (K03, see also Brinchmann et al. 2004). These cata-

³available at <http://www.mpa-garching.mpg.de/SDSS/>

logues are based on the K03 method to infer the star formation histories, dust attenuation and stellar masses of galaxies from the simultaneous analysis of the 4000 Å break strength, $D_n(4000)$, and the Balmer line absorption index $H\delta_A$. These two indices are used to constrain the mean stellar ages of galaxies and the fractional stellar mass formed in bursts over the past few Gyr, and a comparison with broad-band photometry then allows to estimate the extinction and stellar masses.

The MPA/JHU catalogues provide very useful benchmarks for similar studies. In this section we summarize the comparison between values of some of the parameters from these catalogues with our own estimates. A more complete discussion is presented in Cid Fernandes et al. (2005).

Stellar extinction The MPA/JHU group estimates the z -band stellar extinction A_z through the difference between model and measured colours, assuming an attenuation curve proportional to $\lambda^{-0.7}$. In our case, the extinction A_V is derived directly from the spectral fitting, carried out with the Milky Way extinction law (Cardelli et al. 1989, c.f. Section 2.1.). These two independent estimates are very strongly and linearly correlated, with a Spearman rank correlation coefficient $r_S = 0.95$. However, the values of A_z reported by the MPA/JHU group are systematically larger than our values: $A_z(\text{MPA/JHU}) \simeq 2.51A_z(\text{This Work})$ in the median. This discrepancy, however, is only apparent because the Galactic extinction law is substantially harder than $\lambda^{-0.7}$. One thus expects to need less extinction when modeling a given galaxy with the former law than with the latter. Our analysis indicates that there are no substantial differences between the MPA/JHU and our estimates of the stellar extinction other than those implied by the differences in the reddening laws adopted in the two studies.

Stellar masses Our results for the total stellar masses compares very well to the MPA/JHU extinction-corrected stellar masses, with $r_S = 0.89$. The quantitative agreement is also good, with a median difference of just 0.1 dex. This small offset seems to be due to a subtle technicality. Whereas we adopt the M/L ratio of the best χ^2 model, the MPA/JHU group derives M/L comparing the observed values of the $D_n(4000)$ and $H\delta_A$ indices with a library of 32000 models. Each model is then weighted by its likelihood, and a probability distribution for M/L is computed. The MPA/JHU mass is the median of this distribution, which is not necessarily the same as the best- χ^2 value.

Velocity dispersion We use the sub-sample of galaxies with active nuclei to compare our measurements of absorption line broadening due to galaxy velocity dispersion and/or rotation, σ_* , with those of the MPA/JHU group, since they list this quantity only in their AGN Catalogue. The Spearman correlation-coefficient in this case is $r_S = 0.91$ and the median of the difference between the two estimates is just 9 km s^{-1} , indicating an excellent agreement between both studies.

Emission lines and nebular metallicities Brinchmann et al. (2004) also provide, in their Emission line Catalogue, data on emission lines which can be compared with our own measurements. We have compared the fluxes and equivalent widths of $H\alpha$, $[\text{N II}]\lambda 6584$, $[\text{O II}]\lambda 3727$, $H\beta$ and $[\text{O III}]\lambda 5007$ as measured by our code

and that obtained by the MPA/JHU group. We do not find any significant difference between these values; the largest discrepancy (~ 5 per cent) was found for the equivalent widths of $H\alpha$ and $[N\ II]$, probably due to different estimates of the continuum level and the associated underlying stellar absorption. Our emission line measurements are also in good agreement with those in Stasińska et al. (2004), who fit the Balmer lines with emission and absorption components, instead of subtracting a starlight model.

Overall, we conclude that our spectral synthesis method yields estimates of physical parameters in good agreement with those obtained by the MPA/JHU group, considering the important differences in approach and underlying assumptions.

4. Empirical relations

Yet another way to assess the validity of physical properties derived through a spectral synthesis analysis is to investigate whether this method yields astrophysically reasonable results. In this section we follow this empirical line of reasoning by comparing some results obtained from our synthesis of SDSS galaxies (which excludes emission lines) with those obtained from a direct analysis of the emission lines. Our aim here is to demonstrate that our synthesis results do indeed make sense.

4.1. Stellar and Nebular Metallicities

Our spectral synthesis approach yields estimates of the mean metallicity of the stars in a galaxy, $\langle Z_\star \rangle$. The analysis of emission lines, on the other hand, gives estimates of the present-day abundances in the warm interstellar medium. Although stellar and nebular metallicities are not expected to be equal, it is reasonable to expect that they should roughly scale with each other.

Fig. 2 shows the correlation between mass-weighted stellar metallicities and the nebular oxygen abundance (computed as in Section 3.4.), both in solar units⁴, for our sample of normal star-forming galaxies. A correlation is clearly seen, although with large scatter ($r_S = 0.42$). Galaxies with large stellar metallicities also have large nebular oxygen abundances; galaxies with low stellar abundances tend to have smaller abundances. The observed scatter is qualitatively expected due to variations in enrichment histories among galaxies.

Nebular and stellar metallicities are estimated through completely different and independent methods, so the correlation depicted in Fig. 2 provides an *a posteriori* empirical validation for the stellar metallicity derived by the spectral synthesis. The possibility to estimate stellar metallicities for so many galaxies is one of the major virtues of spectral synthesis, as it opens an important window to study the chemical evolution of galaxies and of the universe as a whole (Panter et al. 2004; Sodr e et al. in prep.).

⁴The solar unit adopted for the nebular oxygen abundance is $12 + \log(O/H)_\odot = 8.69$ (Allende Prieto, Lambert & Apslund 2001).

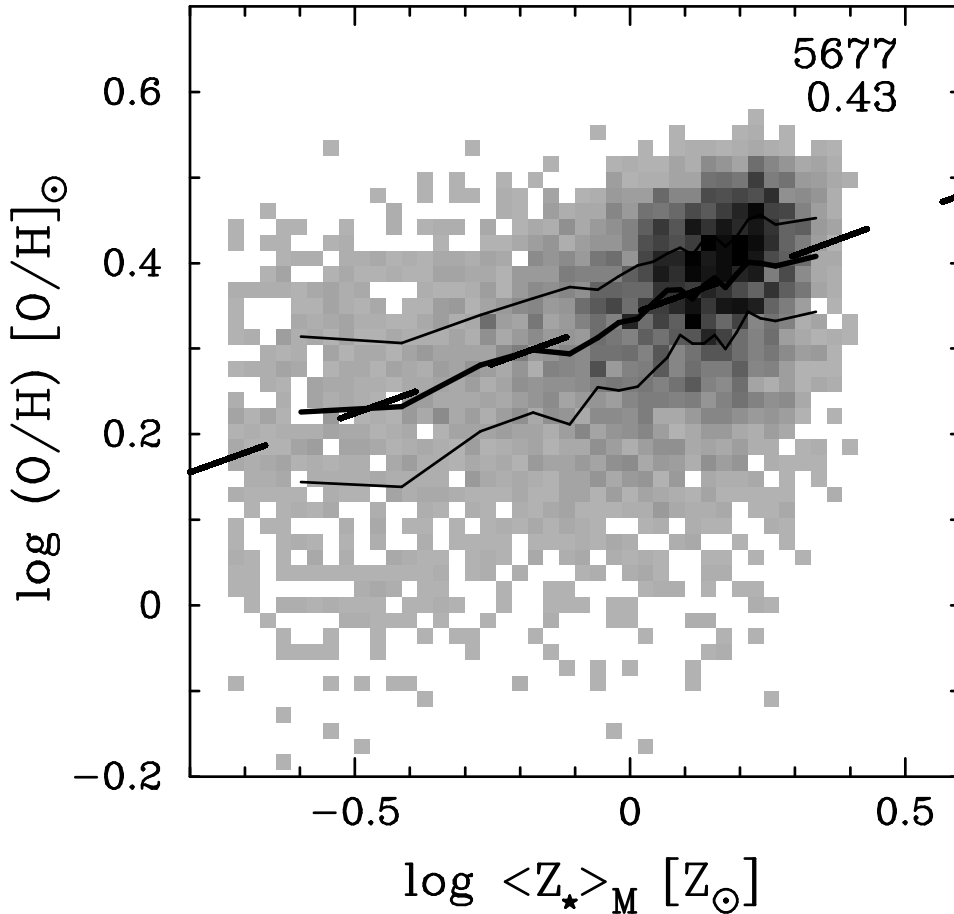


Figure 2. Nebular oxygen abundance versus mass-weighted stellar metallicity, both in solar units, for normal star-forming galaxies in our sample. The median values and quartiles in bins of same number of objects are shown as thin solid lines. The dashed line is a robust fit for the relation.

4.2. Stellar and Nebular extinctions

The stellar extinction in the V-band is one of the products of our STARLIGHT code. A more traditional and completely independent method to evaluate the extinction consists of comparing the observed $H\alpha/H\beta$ Balmer decrement to the theoretical value, the “Balmer extinction” (e.g., Stasińska et al. 2004).

Fig. 3 presents a comparison between the stellar A_V and A_V^{Balmer} . These two extinctions are determined in completely independent ways, and yet, our results show that they are closely linked, with $r_S = 0.61$. A linear bisector fitting yields $A_V^{\text{Balmer}} = 0.24 + 1.81A_V$. Note that the angular coefficient in this relation indicates that nebular photons are roughly twice as extinguished as the starlight. This “differential extinction” is in very good qualitative and quantitative agreement with empirical studies (Fanelli et al. 1988; Calzetti, Kinney & Storchi-Bergmann 1994; Gordon et al. 1997; Mas-Hesse & Kunth 1999).

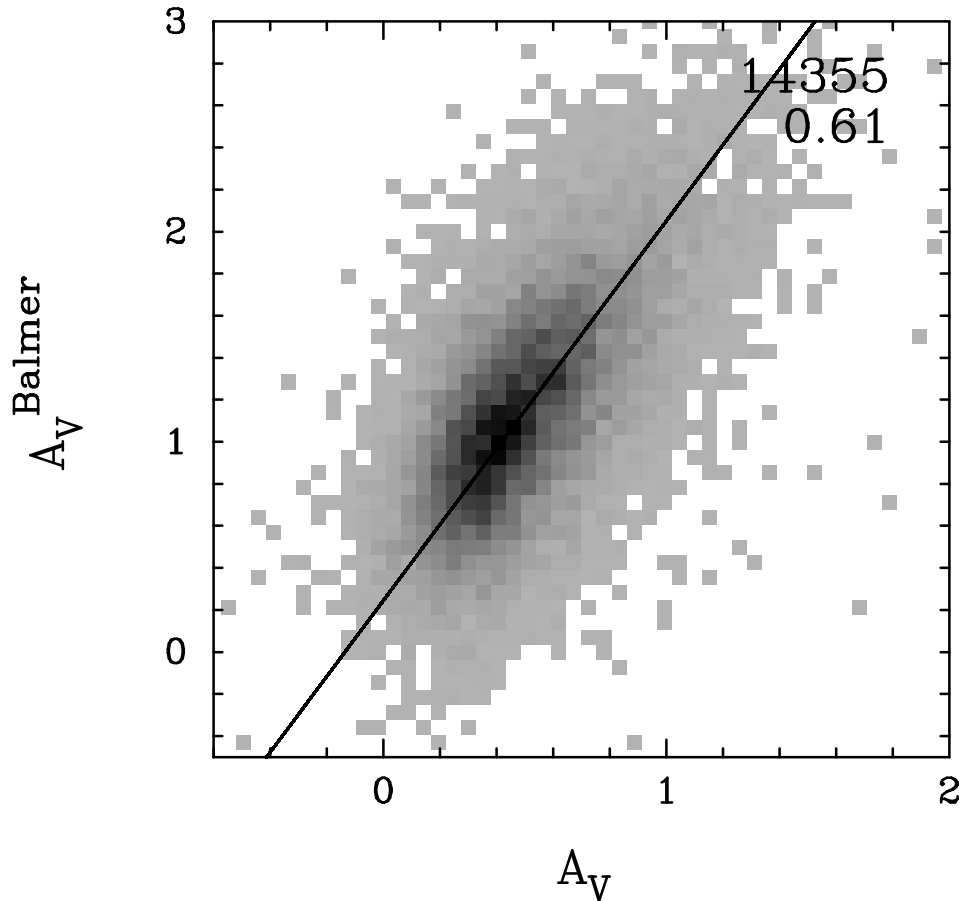


Figure 3. Relation between the nebular (A_V^{Balmer}) and stellar (A_V) extinctions for our sample of normal star-forming galaxies. The solid line is a robust fit for the relation.

4.3. Relations with mean stellar age

The equivalent width (EW) of $H\alpha$ is related to the ratio of present to past star formation rate of a galaxy (e.g., Kennicutt 1998). It is thus expected to be smaller for older galaxies. Fig. 4a shows the relation between $\text{EW}(H\alpha)$ and the mean light-weighted stellar age obtained by our spectral synthesis. The anticorrelation, which has $r_S = -0.78$, is evident. It is worth stressing that these two quantities are obtained independently, since the spectral synthesis does not include emission lines.

Another quantity that is considered a good age indicator, even for galaxies without emission lines, is the 4000 Å break, D4000. We measured this index following Bruzual (1983), who define D4000 as the ratio between the average value of F_ν in the 4050–4250 and 3750–3950 Å bands. The relation between $\langle \log t_\star \rangle_L$ and D4000 is shown in Fig. 4b. Note that the concentration of points at the high age end reflects the upper age limit of the base adopted here, 13 Gyr (c.f. Section 2.2). The correlation is very strong ($r_S = 0.94$), showing that

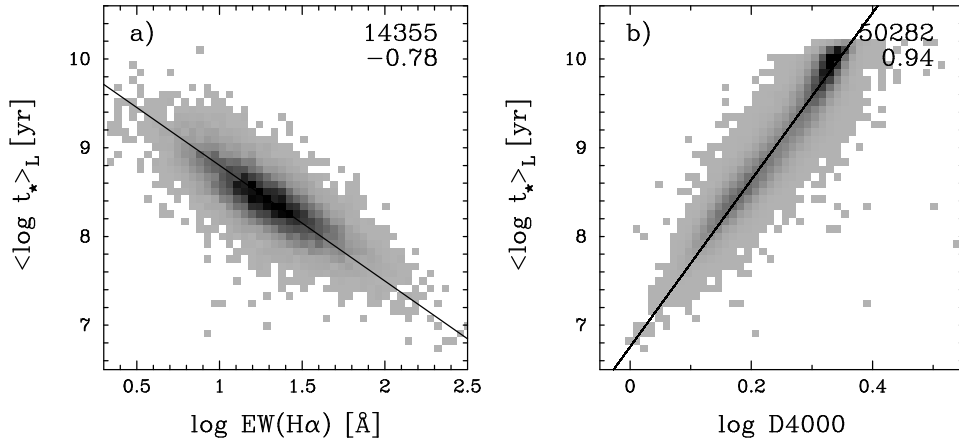


Figure 4. (a) Equivalent width of H α versus the light-weighted mean stellar age for normal emission line galaxies in our sample. (b) Relation between the D4000 index and the light-weighted mean stellar age. The solid lines are robust fits for the relations.

indeed D4000 can be used to estimate empirically mean light-weighted galaxy ages, despite its metallicity dependence for very old stellar populations (older than 1 Gyr, as shown by K03).

4.4. M_\star - σ_\star relation

Fig. 5 shows the relation between stellar mass and σ_\star , obtained from the synthesis. The relation is quite good, with $r_S = 0.79$. The solid line displayed in the figure is $\log M_\star = 6.44 + 2.04 \log \sigma_\star$ for M_\star in M_\odot and σ_\star in km s^{-1} , obtained with a bisector fitting. The figure also shows as a dashed line a fit assuming $M_\star \propto \sigma_\star^4$, expected from the virial theorem under the (unrealistic) assumption of constant mass surface density. In both cases we have excluded from the fit galaxies with $\sigma_\star < 35 \text{ km s}^{-1}$, which corresponds to less than half the spectral resolution of both data and models.

This is another relation that is expected *a priori* if we have in mind the Faber-Jackson relation for ellipticals and the Tully-Fisher relation for spirals. For early-type galaxies, σ_\star is a measure of the central velocity dispersion, which is directly linked to the gravitational potential depth, and, through the virial theorem, to galactic mass. For late-type systems, σ_\star has contributions of isotropic motions in the bulges, as well as of the rotation of the disks, and is also expected to relate with galactic mass. Another aspect that it is interesting to point out in Fig. 5 is that the dispersion in the M_\star - σ_\star relation decreases as we go from low-luminosity, rotation-dominated systems, for which the values of σ_\star depend on galaxy inclination and bulge-to-disk ratio, to high-luminosity, mostly early-type systems, which obey a much more regular (and steeper) relation between σ_\star and M_\star .

This relation, between a quantity that is not directly linked to the synthesis, σ_\star , and another one that is a product of our synthesis, M_\star , is yet another indication that the results of our STARLIGHT code do make sense.

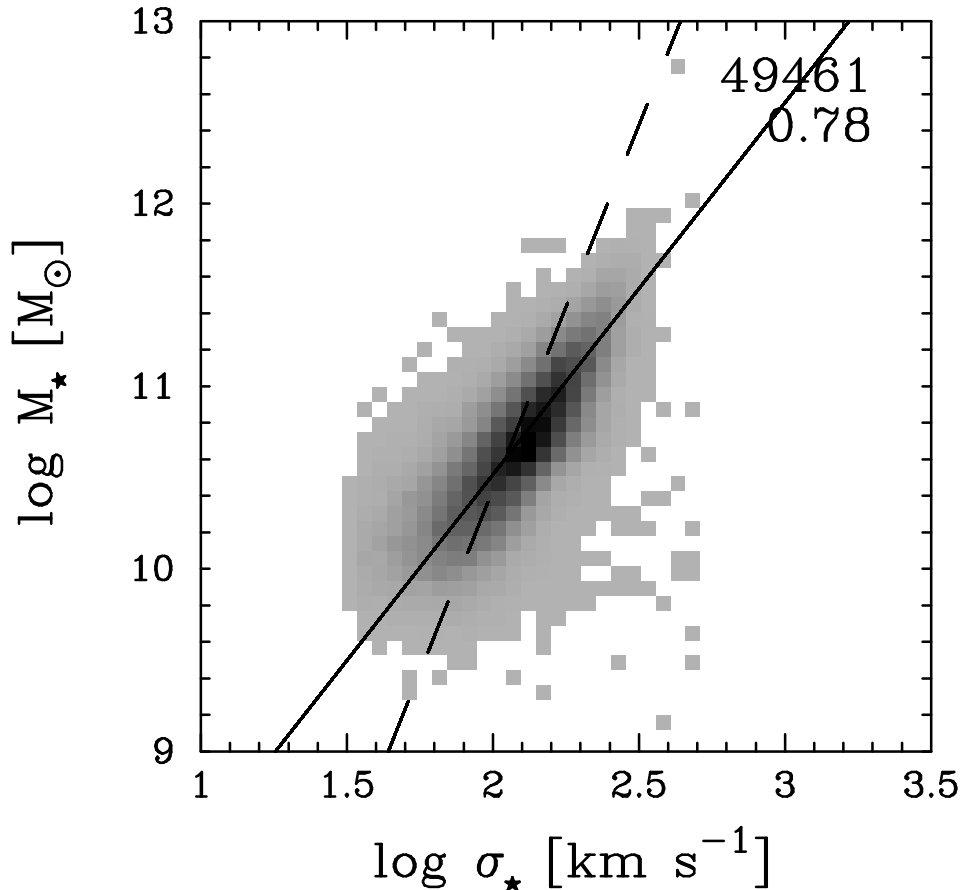


Figure 5. Mass-velocity dispersion relation for our sample. The solid line is a robust fit for the data while dashed one is a fitting assuming $M_{\star} \propto \sigma_{\star}^4$.

5. Recent results

We have started an analysis of a magnitude-limited sample with 20000 galaxies extracted from DR2, aiming to probe galaxies with luminosities smaller than those discussed in the previous sections. We present below a summary of some of the results obtained so far.

The bimodality of galaxy populations With the recent advance of redshift surveys, the study of galaxy populations has quantitatively revealed the existence of a bimodal distribution in some fundamental galaxy properties, found both in photometric and spectroscopic data: star-forming and passive galaxies have quite distinct properties. Perhaps the most representative bimodal distribution is that found in galaxy colours. Since photometric parameters are easily measured, their bimodal behavior has been studied for galaxies in the local universe by using both the SDSS and the Two Degree Field Galaxy Redshift Survey (2dFGRS) data (Strateva et al. 2001; Hogg et al. 2002; Blanton et al. 2003, Wild et al. 2004). A bimodality has been found in other galaxy parameters,

like mass (Kauffmann et al. 2003b) and star formation properties (Madgwick et al. 2002; Wild et al. 2004; Brinchmann et al. 2004). We show in Fig. 6 that the bimodal character of galaxy populations is also clearly present in some parameters derived from our spectral synthesis (Mateus et al., in prep.). These results suggest that galaxies have evolved through two major paths.

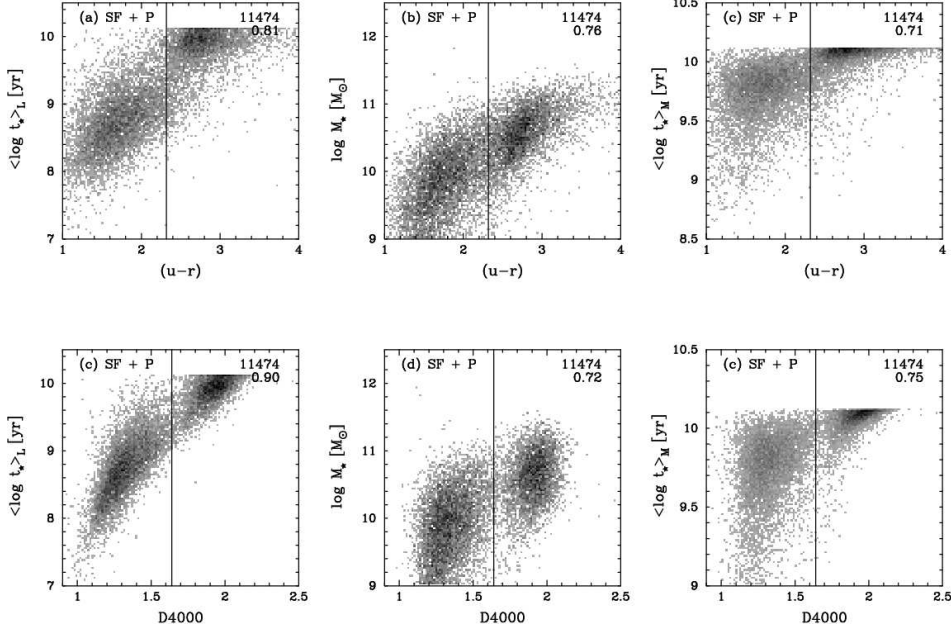


Figure 6. Results of the spectral synthesis of 20000 galaxies of a magnitude-limited sample extracted from SDSS showing properties of star-forming (SF) and passive (P) galaxies. The vertical lines correspond to value of the parameters (colours or $D4000$) which provide the best separation between these two classes of galaxies.

The down-sizing of galaxy populations Another interesting result emerging from our synthesis of SDSS galaxies is the confirmation that there is a correlation between mass and galaxy age, in the sense that most of the stars in massive galaxies were formed long time ago, whereas galaxies with a large fraction of young or intermediate-age stars tend to be less massive. This phenomenon, known as the down-sizing of galaxy populations (Cowie et al. 1996; Juneau et al. 2004; Kodama et al. 2004), is clearly seen in our results with this new sample and, actually, is an essential piece of information on galaxy formation and evolution.

The problem of the alpha-enhancement A major problem of spectral synthesis with a spectral base using BC03 spectra is that while their evolutionary tracks are scaled from the solar values, non-solar abundance patterns may occur in galaxies, mainly in early-types (e.g., Trager et al. 2000a,b). In practice, as discussed by BC03, lines associated to α -elements are not fitted as well as other lines. This problem is indeed present in our results, as shown in Fig. 8 for a subsample of 2488 *bona fide* ellipticals with high S/N spectra. This figure

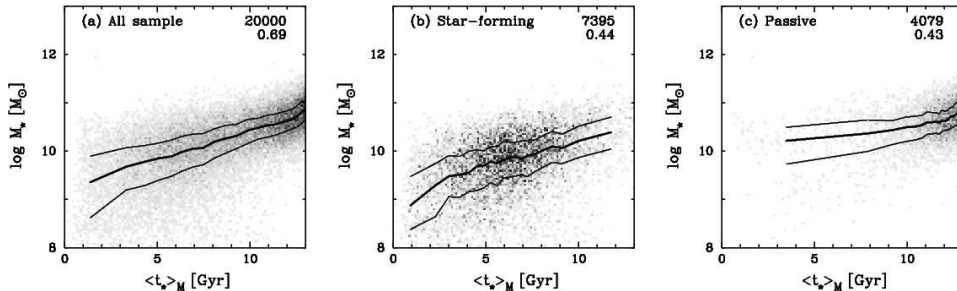


Figure 7. Relation between stellar mass and mean mass-weighted stellar ages for galaxies in the magnitude-limited sample of 20000 galaxies extracted from SDSS.

indicates that the residuals in the absorption lines of some α -elements correlate with the depth of the gravitational potential well of the galaxy (Cid Fernandes et al., in prep.), suggesting that our spectral synthesis results of early-type galaxies may be biased due to inadequacy of the spectral base adopted here to synthesize this type of galaxy.

6. Summary

We have developed and tested a method to fit galaxy spectra with a combination of spectra of individual simple stellar populations generated with state-of-the-art evolutionary synthesis models. The main goal of this investigation was to examine the reliability of physical properties derived in this way. This goal was pursued by three different means: simulations, comparison with independent studies, and analysis of empirical results.

Our simulations show that the individual SSP strengths, encoded in the population vector \vec{x} , are subjected to large uncertainties, but robust results can be obtained by compressing \vec{x} into coarser but useful indices. In particular, physically motivated indices such as mean stellar ages and metallicities are found to be well recovered by spectral synthesis even for relatively noisy spectra. Stellar masses, velocity dispersion and extinction are also found to be accurately retrieved.

We have applied our STARLIGHT code to a volume limited sample of over 50000 galaxies from the SDSS Data Release 2. The spectral fits are generally very good, and allow accurate measurements of emission lines from the starlight subtracted spectrum. We have compared our results to those obtained by the MPA/JHU group (K03; Brinchmann et al. 2004) with a different method to characterize the stellar populations of SDSS galaxies. The stellar extinctions and masses derived in these two studies are very strongly correlated. Furthermore, differences in the values of A_V and M_* are found to be mostly due to the differences in the model ingredients (extinction law). Our estimates of stellar velocity dispersions and emission line properties are also in good agreement with those of the MPA/JHU group.

The confidence in the method is further strengthened by several empirical correlations between synthesis results and independent quantities. We find

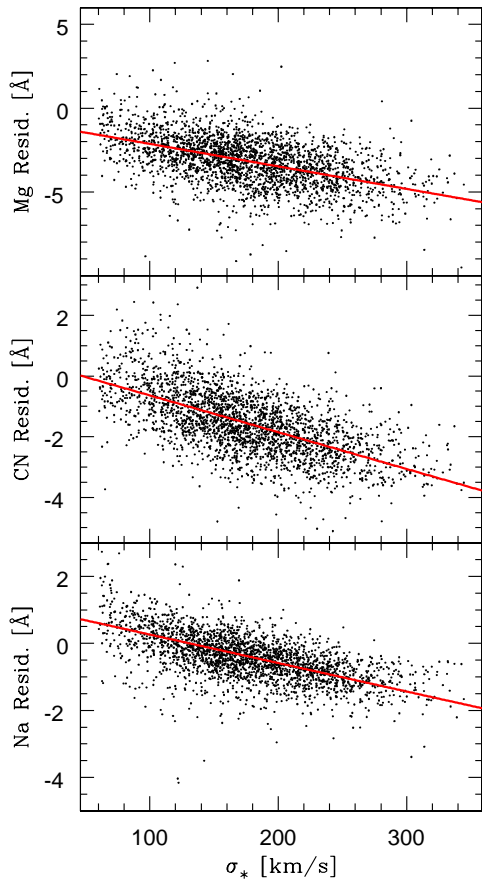


Figure 8. Residuals (measured as equivalent widths) of the spectral synthesis in the region of CN (4132–4196), Mg (5015–5190) and Na D (5874 – 5911) lines as a function of the galaxy velocity dispersion. The data is for a sample of 2488 early-type galaxies.

strong correlations between stellar and nebular metallicities, stellar and nebular extinctions, mean stellar age and the equivalent width of $H\alpha$, mean stellar age and the 4000 Å break, stellar mass and velocity dispersion. These are all astrophysically reasonable results, which reinforce the conclusion that spectral synthesis is capable of producing reliable estimates of physical properties of galaxies. These results validate spectral synthesis as a powerful tool to study the history of galaxies.

We have also presented some preliminary results of an analysis of a magnitude-limited sample containing 20000 galaxies from SDSS which clearly reveal that the bimodality of galaxy populations is present in the parameters obtained from the synthesis. Our results are also consistent with the “down-sizing” scenario of galaxy formation and evolution. Finally, we point out one of the major problems of the spectral synthesis of early-type systems: the spectral base

adopted here is based on solar-scaled evolutionary tracks which may not be appropriate for this type of galaxy.

Acknowledgments

We congratulate D. Valls-Gabaud and M. Chaves for the organization of this workshop. Partial support from CNPq, FAPESP and the France-Brazil PICS program are also acknowledged.

References

- Abazajian, K., et al. 2003, *AJ*, 126, 2081
 Abazajian K. et al. 2004, *AJ*, 128, 502
 Allende Prieto C., Lambert D. L., Asplund M., 2001, *ApJ*, 556, L63
 Baldwin J. A., Phillips M. M., & Terlevich R., 1981, *PASP*, 93, 5
 Bertone, E., Buzzoni, A., Rodríguez-Merino, L. H., & Chávez, M. 2004, *Memorie della Societa Astronomica Italiana*, 75, 158
 Blanton M. R., Brinkmann J., Csabai I., Doi M., Eisenstein D., Fukugita M., Gunn J. E., Hogg D. W., Schlegel D. J., 2003, *AJ*, 125, 2348
 Bressan A., Chiosi C., Tantalò R., 1996, *A&A*, 311, 425
 Brinchmann J., Charlot S., White S. D. M., Tremonti C., Kauffmann G., Heckman T., Brinkmann J., 2004, *MNRAS*, 351, 1151
 Bruzual G., 1983, *ApJ*, 273, 105
 Bruzual G., Charlot S., 2003, *MNRAS*, 344, 1000 (BC03)
 Cardelli J. A., Clayton G. C., Mathis J.S., 1989, *ApJ*, 345, 245
 Calzetti D., Kinney A. L., Storchi-Bergmann T., 1994, *ApJ*, 429, 582
 Chabrier G., 2003, *PASP*, 115, 763
 Cid Fernandes R., Sodr e L., Schmitt H. R., Leão J.R. S., 2001, *MNRAS*, 325, 60
 Cid Fernandes R., Leao J. Lacerda R. R., 2003, *MNRAS*, 340, 29
 Cid Fernandes R., González Delgado R., Storchi-Bergmann, T., Pires Martins, L., Schmitt H., 2004, *MNRAS*, in press (CF04)
 Cid Fernandes R., Mateus A., Sodr e L., Stasińska G., Gomes J. M. 2005, *MNRAS*, 358, 363
 Cowie L. L., Songaila A., Hu E. M., Cohen J. G., 1996, *AJ*, 112, 839
 Fanelli, M.N., O'Connell, R.W., Thuan, T.X., 1988, *ApJ* 334, 665
 Gómez P.L. et al. , 2003, *ApJ*, 584, 210
 González-Delgado, R. M., Cervino, M., Martins, L. P., Leitherer, C., Hauschildt, P. H., 2005, *MNRAS*, 357, 945
 Gordon, K. D., Calzetti, D., & Witt, A. N. 1997, *ApJ*, 487, 625
 Heavens, A., Panter, B., Jimenez, R., & Dunlop, J. 2004, *Nature*, 428, 625
 Hogg D. W. et al., 2002, *AJ*, 124, 646
 Juneau S., et al., 2004, *ApJ*, (astro-ph/0411775)
 Kauffmann G. et al. , 2003a, *MNRAS*, 341, 33 (K03)
 Kauffmann G. et al. , 2003b, *MNRAS*, 341, 54
 Kennicutt R. C. Jr., 1998, *ARA&A*, 36, 189
 Kodama T., et al., 2004, *MNRAS*, 350, 1005
 Le Borgne J.-F. et al. , 2003, *A&A*, 402, 433
 Le Borgne, D., Rocca-Volmerange, B., Prugniel, P., Lançon, A., Fioc, M., & Soubiran, C. 2004, *A&A*, 425, 881
 Mas-Hesse, J. M., & Kunth, D. 1999, *A&AS*, 349, 765
 Madgwick D., et al. (The 2dFGRS Team), 2002, *MNRAS*, 333, 133.
 Panter, B., Heavens, A. F., & Jimenez, R. 2004, *MNRAS*, 458
 Prugniel, P. & Soubiran, C. 2001, *A&A*, 369, 1048

- Renzini A., Buzzoni A., 1986, in Chiosi C., Renzini A., eds, Spectral Evolution of Galaxies. Riedel, Dordecht, p. 213
- Ronen, S., Aragon-Salamanca, A., & Lahav, O. 1999, MNRAS, 303, 284
- Schlegel D. J., Finkbeiner D. P., Davis M., 1998, ApJ, 500, 525
- Schmidt, A. A., Copetti, M. V. F., Alloin, D., & Jablonka, P. 1991, MNRAS, 249, 766
- Searle, L. 1986, in Stellar Populations, ed. C. A. Norman, A. Renzini & M. Tosi (Cambridge, CUP), 3
- Stasińska G., Mateus A., Sodr  L., Szczerba R., 2004, A&A, 420, 475
- Stoughton C. et al., 2002, AJ, 123, 485
- Strateva I., et al., 2001, AJ, 122, 1861
- Strauss, M. A., et al. 2002, AJ, 124, 1810
- Trager, S. C., Faber, S. M., Worthey, G., Jes s Gonz lez, J. 2000a, ApJ, 119, 1645
- Trager, S. C., Faber, S. M., Worthey, G., Jes s Gonz lez, J. 2000b, ApJ, 120, 165
- Tremonti, C. A. et al., 2004, ApJ, 613, 898
- Vazdekis, A. 1999, ApJ, 513, 224
- Wild V., et al., 2005, MNRAS, 356, 247
- Worthey G., 1994, ApJS, 94, 687
- York, D. G., et al. 2000, AJ, 120, 1579
- Zaritsky D., Zabludoff A. I., Willick J. A., 1995, AJ, 110, 1602